Hindawi
Security and Communication Networks
Volume 2022, Article ID 9792724, 1 page
https://doi.org/10.1155/2022/9792724

Retraction

Retracted: Modeling and Control of Wind Speed in Renewable Energy Power Generation and Wind Power Generation Systems

Security and Communication Networks

Received 10 November 2022; Accepted 10 November 2022; Published 21 November 2022

Security and Communication Networks has retracted the article titled "Modeling and Control of Wind Speed in Renewable Energy Power Generation and Wind Power Generation Systems" [1] due to concerns that the peer review process has been compromised.

Following an investigation conducted by the Hindawi Research Integrity team [2], significant concerns were identified with the peer reviewers assigned to this article; the investigation has concluded that the peer review process was compromised. We therefore can no longer trust the peer review process, and the article is being retracted with the agreement of the Chief Editor.

References

[1] J. Shan, S. Lu, S. Liu, and H. Shi, "Modeling and Control of Wind Speed in Renewable Energy Power Generation and Wind Power Generation Systems," *Security and Communication Networks*, vol. 2022, Article ID 6982374, 13 pages, 2022.

[2] L. Ferguson, "Advancing Research Integrity Collaboratively and with Vigour," 2022, https://www.hindawi.com/post/advancing-research-integrity-collaboratively-and-vigour/.

Hindawi
Security and Communication Networks
Volume 2022, Article ID 6982374, 13 pages
https://doi.org/10.1155/2022/6982374

Research Article

Modeling and Control of Wind Speed in Renewable Energy Power Generation and Wind Power Generation Systems

Junwei Shan,[1] **Shixuan Lu**,[2] **Shu Liu**,[3] **and Hang Shi**[2]

[1]*School of Chemical Process Automation, Shenyang University of Technology, Shenyang 110000, Liaoning, China*
[2]*School of Electric Power, Shenyang Institute of Engineering, Shenyang 110000, Liaoning, China*
[3]*School of New Energy, Shenyang Institute of Engineering, Shenyang 110000, Liaoning, China*

Correspondence should be addressed to Junwei Shan; 18403053@masu.edu.cn

Received 6 April 2022; Revised 12 May 2022; Accepted 20 May 2022; Published 10 June 2022

Academic Editor: Mohammad Ayoub Khan

Wind energy is one of the most used clean energy sources in renewable energy, and its renewable and sustainable nature is one of the reasons why it is used for power generation. In the current environment where all countries in the world are facing energy problems, research on wind power generation systems is also increasing. This article aims to study the problem of modeling and controlling wind speed in the wind power generation system of renewable energy power generation. To this end, this article proposes a modeling method for wind power generation systems, which can be used to study the momentum problems in wind power generation and the mechanical torque of the generator. And at the end of the article, related experiments and analysis are designed to explore and compare its operating cost, speed, and wind wheel speed. The experimental results in this paper show that through effective modeling and control of its wind speed, the economic risks in the actual wind power generation system can be controlled, with a maximum reduction of 24%, and the actual operating cost is also reduced by 8.66%, so wind power has high practical value.

1. Introduction

In China, the proportion of wind power generation in the power system is gradually increasing. As a clean energy, wind energy is very important in changing the existing energy structure and promoting national economic and social development. Today, wind power generation faces many problems, including various types of wind turbines, harsh wind farm environment, low technical level of operators, and single function of existing monitoring systems. At present, in the production management of modern wind power enterprises, in order to achieve the goal of remote centralized monitoring and unmanned wind power stations, a comprehensive monitoring and management platform for various wind turbines and booster stations is required. Wind power companies are moving toward centralized development, providing a monitoring system with rich reporting types, intuitive graphical data analysis, and hopefully providing the data and technical foundation to further enable early warning systems for wind turbine failures.

China is rich in wind energy reserves, whether it is land wind energy or offshore wind energy; the potential that can be developed and tapped is very large. Because wind energy itself is rich in reserves and easy to exploit, it is better than fossil energy when it is utilized. Compared with fossil energy and hydropower, which is also a clean energy, wind energy will not produce any harmful substances in the production process, and its development will cause much less damage to the ecological environment than hydropower. Therefore, vigorously developing wind power is of great significance to meet China's energy demand, reduce environmental pollution, change the existing energy structure, and promote national economic and social development.

The innovation of this paper is that based on the theoretical basis of wind power generation system, combined with the modeling method of wind power generation, the relevant research is carried out, and the characteristics of the process of renewable energy power generation are analyzed in detail, so that the improved modeling method of the article is carried out, which can be more targeted and efficient.

2. Related Work

With the rapid development of the world, after the international environmental protection organization proposed a green and low-carbon life, all countries in the world are actively responding to its call. More and more attention has been paid to the power generation of renewable energy, and more and more people have begun to invest in this research. Balezentis believes that the integrated assessment model (IAM) is ubiquitous in energy policy analysis. Although IAMs can successfully handle the uncertainty associated with energy planning problems, they still take multiple variables as the output of the modeling. As a result, policymakers are faced with multiple energy development scenarios and goals. Specifically, technical, environmental, and economic aspects are represented by multiple criteria, which in turn are related to conflicting goals [1]. Xie proposed that the power oscillation caused by the interaction between the power converter and the AC/DC grid is an important stability problem faced by the grid-connected renewable energy generation system (GREGS). Small-signal modeling is fundamental to analyzing such problems. But the large number of converters with different structures, parameters, and "black (grey) box" control systems makes it difficult for conventional methods to deal with the system modeling problem. A small-signal impedance (admittance) network modeling approach is proposed to address this problem [2]. Li discussed the Hamiltonian mathematical modeling and dynamic analysis of hydropower systems under transient load increases. First of all, six kinds of dynamic transfer coefficients of turbine transient load abrupt change are innovatively introduced into the hydropower generation system. Considering the elastic water hammer model of the pressure pipeline and the third-order model of the generator, the dynamic mathematical model of the hydroelectric power generation system under the load surge transient is established [3]. Lozano used ecoefficiency as a tool to compare the two options, based on 1000 kg/h of residual pecan shell residue, the stream of chemicals that can be produced, and the electricity that can be produced by gasification of residual biomass [4]. Lisboa proposes an analytical scheduling of tidal power plants concentrating discharge periods under tidal extremes. Since the tidal cycle is well predicted by the sine function, the method provides accurate power generation, as shown in the comparative tests. Furthermore, considering that all stored water is discharged during tidal extremes, at the maximum head, the optimal power generation estimation method is derived [5]. Lohse will presents studies with the goal of evaluating hydrogeothermal power generation and heat generation in low-enthalpy regions from an environmental perspective. The German Environment Agency publishes the results of a web-based study that analyzed the detailed and comprehensive environmental impacts of geothermal power generation in Germany between 2008 and 2016 and continuously evaluates these findings. He discusses the results of a life cycle assessment, taking into account all impacts and material flows throughout the life cycle [6]. Rajarathinam investigated the power harvested from the hybrid collector under harmonic excitation using experimental and analytical evaluations. Comparisons were made with stand-alone piezoelectric and electromagnetic harvesters under similar excitation environments. Studies have shown that current hybrid harvesters can harvest energy in a wide frequency range. In addition, some parametric studies are also carried out to understand the device output performance [7]. Islam used the WtE strategy to assess the renewable energy potential and climate benefits of MSW from urban waste management in Bangladesh through carbon reduction. The study is based on waste generation in seven major urban companies, 308 cities and 208 other urban areas in Bangladesh. The energy potential of different WtE strategies was assessed using standard energy transition models and subsequent greenhouse gas (GHG) emission models [8]. The literature mainly focuses on the exploration of energy power generation. There is a very detailed introduction to the related power generation technology, power generation process and equipment, but the introduction of the wind power generation system is still too little, and modeling related content is also not carried out.

3. Wind Power Generation System Modeling Method

3.1. Wind Power System

3.1.1. Fixed Speed and Variable Speed Wind Turbines. Wind turbines can run either at fixed speed or at variable speed. For fixed-speed wind turbines, the generators are directly connected to the power grid. Since the speed of the generator needs to match the frequency of the power grid, it cannot control the speed, nor can it store the rotational kinetic energy caused by the change of wind speed. Therefore, for fixed-speed wind turbines, the fluctuation of wind speed will bring about changes in output power, thus affecting the power quality of the power grid. For variable-speed wind turbines, the speed of the generator can be controlled by the power electronic equipment, and the power fluctuation caused by the change of wind speed can be absorbed by the speed of the motor, thereby smoothing the electric power input to the grid. Therefore, compared with the fixed-speed wind turbine, the power quality of the output power of the variable-speed wind turbine has been greatly improved.

Based on these reasons, the current mainstream in the wind power industry is the variable speed wind turbine, which is also the model discussed in this paper.

3.1.2. Stall type and Pitch Type Wind Turbines. The force acting on a rotor blade is a function of wind speed, rotational speed, and blade angle, which determine the blade's angle of attack. Based on these three elements, different control strategies are formed.

(1) Stall control: when the blade angle of the fan blade is fixed (that is, when the blade is fixed on the hub), only the stall effect controls the power captured by the blade. In this configuration, only the nominal

wind speed can reach the rated power, and the main advantage is that the blades are fixedly connected to the hub, which is highly stable and economical [9]. The disadvantage is that the power output over the entire wind speed operating range needs to be determined in advance. Even in the presence of sufficient wind energy, the fan cannot produce rated power. This condition can be caused by a variety of conditions, the most common being that the wind speed in operation is higher than the nominal wind speed. It may also be that dirt on the blade surface reduces its aerodynamic performance. Finally, changes in air density, air pressure, and temperature will affect the available power in wind energy, and stall-type wind turbines cannot effectively cope with these changes [10].

(2) Active stall control: in order to make the wind turbine always generate rated power when there is available wind energy, active stall control can be used. This meteorological control method is also called combined stall control. Under this control strategy, the wind turbine performs fine pitching in the high wind speed period to obtain the required rated power and makes better use of the wind turbine system. And after adopting this control strategy, in the high wind speed period, the power curve of the wind turbine is very gentle due to the change of wind speed [11]. Another significant advantage is that it makes it easier to start and stop the wind turbine. The disadvantage is that the connection between the blade and the hub needs to be very flexible.

(3) Pitch control: pitch control is similar in principle to active stall control, in which the blades capture the required power by pitching. The goal of this strategy is to maintain a proper air layer around the blade throughout the entire wind speed operating range, which can reduce unnecessary longitudinal loads on the system and allow the blade angle to vary within a wider range [12]. The advantage is also better utilization of the wind turbine system. In addition, the load acting on the wind turbine can be reduced. At present, some data show that the load on the pitch control wind turbine at the maximum wind speed is only 1/3 of the stall regulation wind turbine. The disadvantage is that the pitch control system needs to be installed, which increases the failure rate and maintenance costs. In addition, small wind speed changes will lead to large power fluctuations, and the pitch system does not respond quickly to these power changes [13].

3.1.3. Key Components and Electromechanical Conversion Systems. As a large system, a wind turbine contains many conversion components (conversion components that convert wind energy into mechanical energy and mechanical energy into electrical energy).

Figure 1 shows the main components of a typical wind turbine. There may be differences in individual components in other types of wind turbines, especially direct-drive (gearboxless) wind turbines, but the diagram can still be used as a general reference to help understand wind turbine construction [14].

Additionally, there are components that are not directly involved in the power conversion system, which play an important role in ensuring the normal, efficient, and reliable operation of the system, including pitch systems, yaw control systems, mechanical brakes, wind speed/direction sensors, and towers. The electromechanical conversion systems are mainly generators and converters [15].

Large-scale wind turbines need to be developed to capture wind energy to the greatest extent but have long been limited by power converters. The concept of a doubly-fed asynchronous wind turbine achieves this breakthrough. The stator winding of this generator is directly connected to the grid, and the rotor winding is connected to the grid through back-to-back power converters, and the capacity is only 25% of the rated capacity of the generator. Doubly-fed asynchronous generators run in the range of 30% of the synchronous speed, which can meet the normal operation requirements under most wind speed conditions [16]. At the same time, the DFIG can also realize the decoupling control of active and reactive power. Due to the characteristics of low price and small space occupation of the matching converter, the DFIG asynchronous wind power generation system is the most popular product in the wind power market and is widely used in every wind turbine manufacturer and newly built wind farms, and the capacity can reach 3.5 MW. Another type of asynchronous motor is the squirrel-cage asynchronous motor, which cannot be connected to the rotor side. Because it uses a full-power power converter, almost only Siemens is still producing it. In contrast, the cage-type asynchronous wind turbine has the characteristics of simple structure and robustness, which not only is cheap, but also requires the least maintenance. According to the long-term tradition of generator design and production, the use of wound asynchronous motors is used in the field of wind power. This type of model is mainly used by Germany's Enercon Company and Croatia' *s* KONCAR wind turbine manufacturer. Despite the many debates about the price of permanent magnets, many forecasts suggest that PM synchronous wind turbines will be the mainstream trend, and most wind turbine manufacturers say that recent R&D and investment have been concentrated in this area, compared to DFIG and PMSM both having higher efficiency and higher power density [17]. At the same time, in order to have a better understanding of the wind situation, most enterprises will use simulation to simulate the risk, so as to obtain better data for a detailed grasp of it. Figure 2 shows the simulation system structure.

The main difference between the asynchronous motor and the synchronous motor in the wind power field is that the asynchronous motor rotates at high speed and requires a gearbox, while the low-speed rotation of the synchronous motor is suitable for the concept of direct drive. The requirement for high-speed rotation of asynchronous motors is due to the manufacturing factors of this type of motor and its mandatory cylindrical rotor with only a small number of poles installed [18, 19]. In addition, asynchronous motors act as

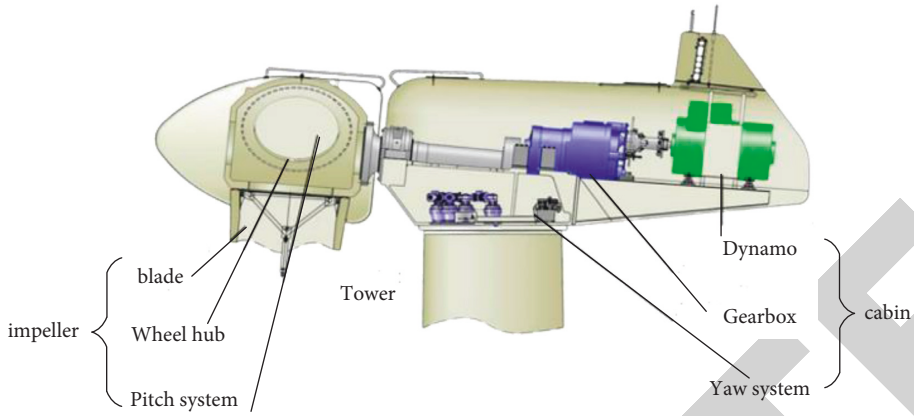

Figure 1: Internal structure of wind turbine.

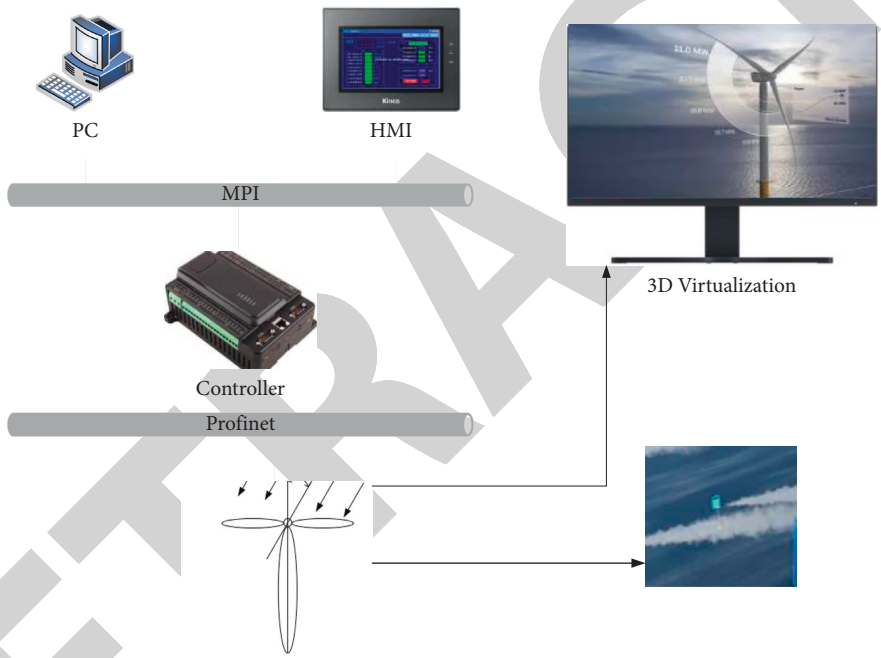

Figure 2: Wind farm simulation system structure.

electromechanical attenuators between variable-speed turbulent wind and constant grid frequency, while synchronous motor wind turbines use power converters to achieve this.

Connecting the wind power system to the grid is a complex task, which relies on AC-DC-AC three-phase full-bridge converters, also known as back-to-back converters. For a long time, the development of large-scale wind turbines has been limited by the technology of large-capacity power converters [20]. So the doubly-fed asynchronous motor was introduced to solve this problem. The cost of power converters currently accounts for 7% of the total cost of wind turbines. Due to the randomness of the wind, the power output of the wind turbine has continuous fluctuations. On the other hand, the grid requires constant frequency power and minimal harmonic distortion. The only way to achieve this is to better design the control structure of the power converter to fully exploit the possibilities of the converter [21, 22].

3.2. Modeling of Wind Power Systems. In the simulation of wind power generation in the power system, the wind speed is assumed to be the sum of four wind volumes (average, slope component, gust component, and turbulence component). The turbulent component is described by the power spectral density. Considering that the turbulence component represents the distribution of wind speed in the frequency domain and the dynamic simulation of the power system is carried out in the time domain, this item is replaced by random noise [23, 24]. New wind speed models are mean value, slope component, gust component, and random wind [25]. Figure 3 shows the wind model for various wind speeds.

$$v_w(t) = v_a(t) + v_r(t) + v_g(t) + v_n(t). \quad (1)$$

The value of wind speed is obtained by superposition of the four components. The ramp component V_r is described

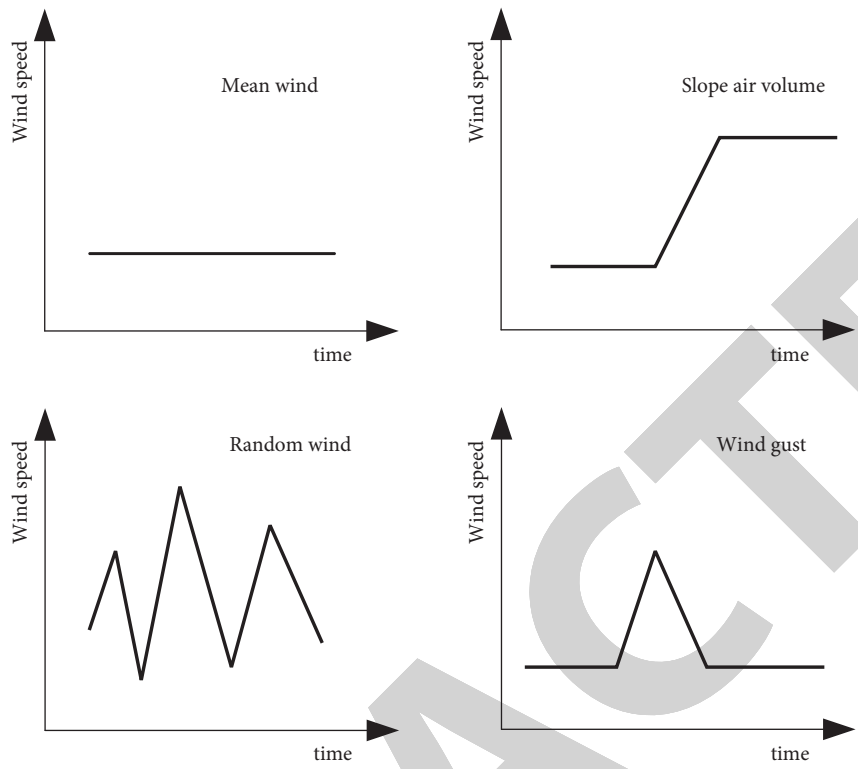

Figure 3: Wind model.

by three parameters: amplitude A_r, start time T_{rs}, and end time T_{re}, as follows:

$$t < T_{rs}, v_r = 0,$$
$$T_{rs} \le t \le T_{re}, v_r = \frac{t - T_{rs}}{T_{re} - T_{rs}}, \quad (2)$$
$$t > T_{re}, v_r = A_r.$$

The gust component is described by V_g with three parameters: amplitude A_g, start time T_{gs}, and end time T_{ge}, as follows:

$$t < T_{gs}, v_g = 0,$$
$$T_{gs} \le t \le T_{ge}, v_g = A_g\left\{1 - \cos\left[2\pi\left(\frac{t - T_{gs}}{T_{ge} - T_{gs}}\right)\right]\right\}, \quad (3)$$
$$t > T_{ge}, v_g = A_g.$$

Random wind is described by one parameter and one function: magnitude A_g, random function (generates random values in the range [−1,1]).

$$v_n(t) = A_n \text{random}(t). \quad (4)$$

The average value of the wind speed, V_a, is called the basic wind.

The wind direction is another important parameter of the wind model. In order to simulate the volatility of the wind direction, the wind direction is divided into the superposition of the main wind direction α_a and the fluctuating wind direction A_a, and the fluctuating wind direction changes according to the sine value, as follows:

$$\alpha(t) = \alpha_\alpha + A_\alpha \cos(t). \quad (5)$$

As shown in Figure 4, the main wind direction setting range is −180°~180°, and the fluctuation range is −5°~+5°.

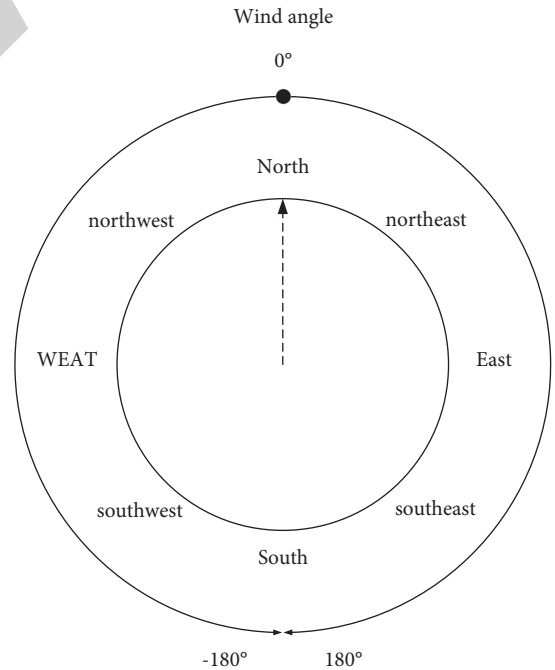

Figure 4: Schematic diagram of wind direction.

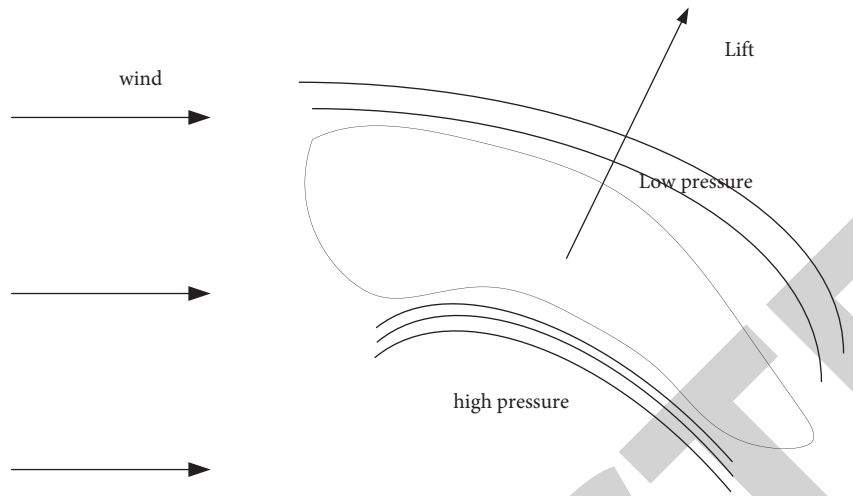

Figure 5: Schematic diagram of blade generating lift.

Due north is the 0° wind direction. Clockwise, the angle increases, and counterclockwise the angle decreases.

The wind wheel model directly determines the efficiency of the wind turbine to obtain energy from the wind [26]. The wind wheel includes the hub and the blades in the wind turbine, and its main function is to convert the wind energy into mechanical energy (mechanical torque) to drive the main shaft of the fan to rotate. When the air flows through the blade, a pressure difference will be generated on the upper and lower sides of the blade, forming a lift force, and the lift force will generate an aeromechanical torque centered on the hub, which will drive the impeller to rotate. Wind energy utilization efficiency is related to wind speed, wind direction, pitch angle, yaw angle, and rotor speed. The simulation methods are also different for different simulation purposes (formula method, table method, and leaf element momentum method). The schematic diagram of the blade generating lift is shown in Figure 5.

According to the one-dimensional momentum theory of an ideal fan, the formula for the power absorbed by the fan from the wind is derived:

$$P = 0.5\rho C_p(\theta, \lambda)\pi R^2 v^3 \cos\alpha. \tag{6}$$

C_p is the utilization efficiency of wind energy, R is the radius of the impeller, V is the wind speed, α is the angle between the nacelle and the wind direction, P is the mechanical power of the fan, and ρ is the air density. By fitting a large amount of data, the formula for C_p can be obtained as

$$C_p(\lambda, \theta) = c_1\left(\frac{c_2}{\lambda_i} - c_3\theta - c_4\theta^{c_5} - c_6\right)e^{(-c_7/\lambda_i)},$$
$$\lambda_i = \left[\left(\frac{1}{\lambda - c_8\theta}\right) - \left(\frac{c_9}{\theta^3 + 1}\right)\right]^{-1}. \tag{7}$$

The coefficient c in the formula will be slightly different according to different fan types. Table 1 shows the power curve changes of the two commercial machines.

The characteristics of the formula method simulation are simple modeling and fast simulation speed, but the disadvantage is that it is only suitable for the normal operation of the fan, is no longer applicable to the simulation of the fan on and off, and cannot be simulated under all conditions. The reason is that when calculating the mechanical torque, the following formula is used:

Table 1: Power curves of two commercial fans.

	Constant speed fan	Variable speed fan
C1	0.44	0.73
C2	125	151
C3	0	0.58
C4	0	0.002
C5	0	2.14
C6	6.94	13.2
C7	16.5	18.4
C8	0	−0.02
C9	-0.002	−0.003

$$T_r = \frac{P}{\omega_r}. \tag{8}$$

Among them, T_r is the mechanical torque, and ω_r is the fan speed. When the fan is on or off, ω_r is 0, and the calculated T_r is infinite, which makes the simulation impossible.

In order to overcome the disadvantage that the formula method is only suitable for steady state, the table method can be used. The formula used in calculating the mechanical torque is as follows:

$$T_r = 0.5\rho C_p(\theta, \lambda)\pi R^3 v^2 \cos\alpha. \tag{9}$$

This method directly calculates T_r by checking the table, so that the simulation of starting and stopping can be carried out, but the disadvantage is that it requires a large amount of experimental data and also needs aerodynamic experimental data corresponding to a specific model, which is not universal enough.

The blade element momentum method is a common model for calculating the mechanical torque of the fan. The table method is to store the actual experimental data in the

table and read the data directly from the table during simulation. The blade element momentum method decomposes the blade into micro elements and finally solves the mechanical moment on the entire blade through integration.

The calculation steps are as follows:

(1) Initializing the axial induction factor a and the lateral induction factor a', usually $a = a' = 0$.

(2) Calculating the inflow angle (the angle between the wind speed relative to the blade and the rotation plane of the blade).

$$\Phi = \arctan\left[\frac{(1-a)v_{\text{wind}}}{(1-a\prime)\omega_r r}\right]. \tag{10}$$

(3) Calculating the local angle of attack, the difference between the inflow angle and the pitch angle.

$$\alpha = \Phi - \theta. \tag{11}$$

(4) Finding the lift coefficient Cl and drag coefficient Cd through the local angle of attack. The relationship between the lift/drag coefficient and the angle of attack is generally obtained through wind tunnel experiments.

$$\begin{aligned} c_l &= \text{Table}(\alpha), \\ c_d &= \text{Table}(\alpha). \end{aligned} \tag{12}$$

(5) Through the decomposition of the force, the lifting force coefficient Ct and the positive pressure coefficient Cn can be calculated.

$$\begin{aligned} c_n &= c_l \cos\Phi + c_d \sin\Phi, \\ c_t &= c_l \sin\Phi - c_d \cos\Phi. \end{aligned} \tag{13}$$

(6) Calculating the axial induction factor a and the lateral induction factor a'.

$$\begin{aligned} a &= \frac{1}{4\sin^2\Phi/\sigma c_n + 1}, \\ a\prime &= \frac{1}{4\sin\Phi\cos\Phi/\sigma c_t - 1}. \end{aligned} \tag{14}$$

(7) Determining whether the change of the axial induction factor a and the lateral induction factor a' is greater than a certain allowable deviation; if it is greater than the deviation, go back to the second step for calculation; otherwise, jump out of the loop

(8) Calculating the local lift force and positive pressure of the blade.

$$\begin{aligned} p_n &= \frac{1}{2}\rho v_{rel}^2 c(r) c_n, \\ p_t &= \frac{1}{2}\rho v_{rel}^2 c(r) c_t. \end{aligned} \tag{15}$$

In

$$v_{rel} = \sqrt{\left[\omega_r r\left(1 + a'\right)\right]^2 + \left[v_{wind}\left(1 - a\right)\right]^2}, \tag{16}$$

is the relative wind speed and is the local chord length.

3.3. Characteristics of Renewable Energy Power Generation. Compared with conventional generator sets such as thermal power, hydropower, and nuclear power, wind power and photovoltaic power generation have many different characteristics, which are mainly reflected in the following aspects.

(1) Wind power and photovoltaic power generation are intermittent and fluctuating. The output of wind turbines varies randomly according to the wind speed and cannot maintain a controllable and constant output. Similarly, the output of photovoltaic power plants is affected by the intensity of solar radiation, and it cannot maintain a controllable and constant output, which is the biggest disadvantage of wind power and photovoltaic power generation. From the perspective of power supply reliability, wind power and photovoltaic power generation only provide electricity and cannot provide capacity matching their installed capacity.

(2) The annual utilization hours of wind power and photovoltaic power generation are relatively low. The utilization hours of wind power equipment are mainly determined by wind energy resources, which depend on the size and distribution of wind energy resources, and are also affected by grid constraints. In recent years, the large-scale development of wind power has made it difficult to connect to the grid in some areas, and the power generation output is limited. During the "Twelfth Five-Year Plan" period, the utilization hours of wind power equipment are about 2000h. The fractional utilization of solar photovoltaic power generation equipment is completely affected by the solar irradiation time, and there are very obvious differences in different regions. In areas with abundant solar energy resources in China, the utilization hour of photovoltaic power generation is expected to be 1500h. Several common renewable energy power generations are shown in Figure 6.

At present, electric energy cannot be stored in a large amount, so the generation and consumption of electricity are synchronized, and the amount of electricity generated on the generation side is determined by the required electricity consumption. The power load of the power grid has been fluctuating. In order to keep the active power of the system in balance and maintain the frequency stability, the power generation side needs to adjust the generator output synchronously to adapt to the load fluctuation. Compared with conventional energy sources such as hydropower and thermal power, wind power and photovoltaic power generation have the characteristics of unstable output, intermittent and fluctuating nature, low prediction accuracy, and low capacity reliability. The state supports clean energy, and

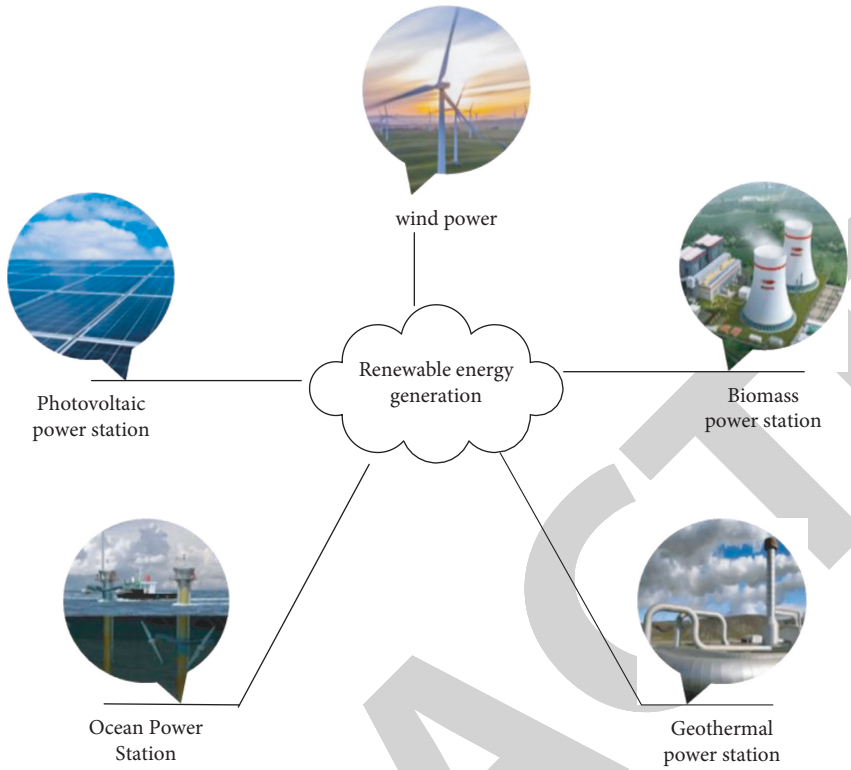

Figure 6: Several common renewable energy power generations.

the output of wind power and photovoltaic power generation gives priority to the Internet. Therefore, in order to ensure that the output of wind power and photovoltaic power generation is always connected to the Internet, not only the daily peak regulation demand of the system is the load peak-valley difference before the connection of wind power and photovoltaic power generation, but also many factors need to be taken into consideration (wind power and photovoltaic power generation access capacity).

The output of wind power and photovoltaic power generation is fluctuating, uncertain, and intermittent. It is an unstable power supply to the power system, which is equivalent to a negative load. Its changes need to be balanced by other generator sets in the power grid, and photovoltaic power generation shows the opposite peak shaving effect.

The impact of renewable energy power generation on the peak-to-valley difference of system load depends on the relationship between the range and direction of daily output changes of wind power and photovoltaic power generation and the magnitude and direction of load changes. According to the different change patterns of wind power and photovoltaic power generation on the net load peak-to-valley difference of the grid, the peak regulation effect is divided into three situations: negative peak regulation, positive peak regulation, and over peak regulation. Antipeak regulation refers to the fact that the daily output increase and decrease trend of renewable energy is opposite to the system load curve, and the peak-valley difference of the system net load curve increases after the output of renewable energy is connected. Positive peak shaving means that the daily output increase and decrease trend of renewable energy is basically the same as the system load, the peak-to-valley difference of renewable energy output is smaller than the peak-to-valley difference of system load, and the peak-to-valley difference of the net load curve of the system decreases after the renewable energy is connected. Over-peak regulation means that the daily output increase and decrease trend of renewable energy is basically the same as the system load, the peak-to-valley difference of renewable energy output is greater than the peak-to-valley difference of system load, and the peak-to-valley curve of system net load is inverted after renewable energy is connected.

4. Experiment of Power Generation Optimization Effect in Power System

Algorithm example verification: in order to verify the performance and optimization effect of the algorithm proposed in this paper in solving the power system generation planning optimization problem and to compare with the calculation results in the related literature, this paper uses the IEEE 10-generator system as an example to analyze the algorithm. The algorithm program is written in MATLAB language and debugged and run on a personal computer.

The basic parameters of the IEEE-10 unit system are shown in Table 2.

In the table, $T_i^{on}, T_i^{off}, T_i^{cs}$ are the minimum continuous operation time, outage time, and cold start time of unit i. "Initial state" is the continuous operation time before the unit scheduling cycle, and a negative value indicates the continuous outage time.

Table 2: System unit parameters.

Unit number	T_i^{on}	T_i^{off}	T_i^{cs}	Initial state (h)
G1	8	8	5	8
G2	8	8	5	8
G3	5	5	4	-5
G4	5	5	4	-5
G5	6	6	4	-6
G6	3	3	2	-3
G7	3	3	2	-3
G8	1	1	0	-1
G9	1	1	0	-1
G10	1	1	0	-1

Table 3: System load power.

t	$P_{D,t}^f$	t	$P_{D,t}^f$	t	$P_{D,t}^f$	t	$P_{D,t}^f$
1	700	7	1150	13	1400	19	1200
2	750	8	1200	14	1300	20	1400
3	850	9	1300	15	1200	21	1300
4	950	10	1400	16	1050	22	1100
5	1000	11	1450	17	1000	23	900
6	1100	12	1500	18	1100	24	800

Table 4: Economic comparison of units.

Unit number	$\mu_{i,\min}$	$\mu_{i,\min}/P_{i,\min}$	Priority 1	Priority 2
G1	18.61	0.041	1	1
G2	19.53	0.043	2	2
G3	22.24	0.171	4	5
G4	22.01	0.169	3	4
G5	23.12	0.143	5	3
G6	27.45	0.343	6	6
G7	33.45	0.394	7	7
G8	38.15	0.694	8	8
G9	39.48	0.718	9	9
G10	40.07	0.728	10	10

Table 5: Comparison of convergence results between the algorithm in this paper and related intelligent algorithms.

Algorithm	Total power generation cost/$			Average calculation time/s
	The optimal value	Worst value	Average value	
GA	565825	590032	—	221
PSO	563977	564986	564487	—
QEA-UC	563938	564672	563969	15
QBPSO	563977	563977	563977	18
Algorithm	563938	563977	563940	19

The predicted load power in the system scheduling period is shown in Table 3.

For the economic priorities of units under different optimization objectives, different parameters can be selected as the basis for ranking according to the technical economy and load characteristics of the units. In the optimization model of power generation planning, the optimization objective is to minimize the overall energy consumption of the system, so the energy consumption characteristics of the units are selected as the basis for sorting. The traditional index based on energy consumption is the minimum specific consumption, that is, the minimum average coal consumption per unit of electricity, but when some units are not operating near their rated value, it is not economical to sort by the minimum specific consumption. Therefore, in this example, the ratio of the minimum specific consumption and the maximum output of the unit is used as the economic ranking index of the unit, as shown in "Priority 2" in Table 4.

The algorithm proposed in this paper is independently operated for 20 times, and the optimal convergence result of

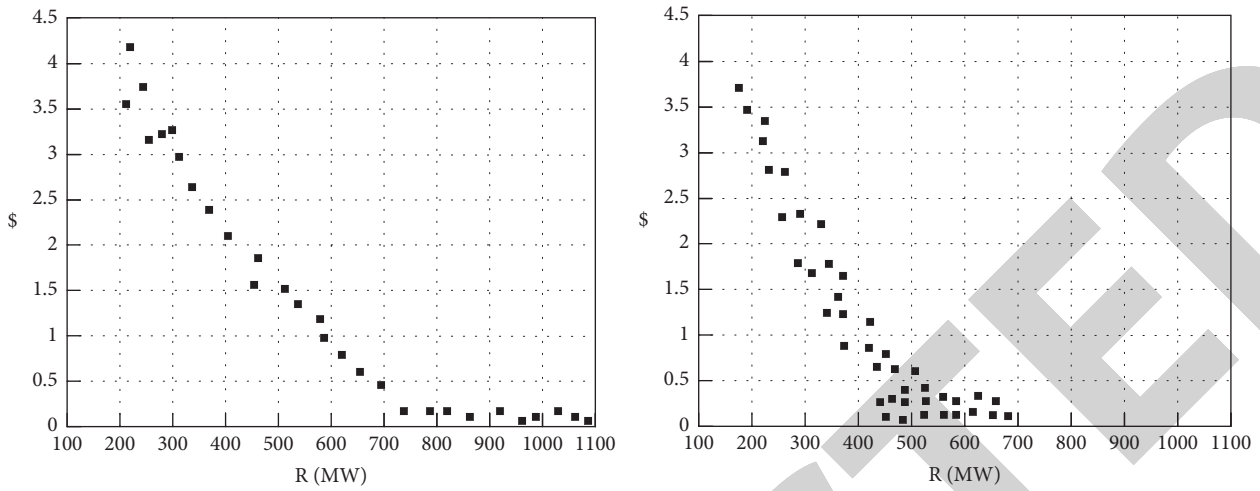

Figure 7: Comparison of power balance risk metrics with positive spinning and negative spinning reserve capacity.

unit	Start and stop status of the unit every hour																							
	1	2	3	4	5	6	7	8	9	10	11	12	13	14	15	16	17	18	19	20	21	22	23	24
G1	■	■	■	■	■	■	■	■	■	■	■	■	■	■	■	■	■	■	■	■	■	■	■	■
G2	■	■	■	■	■	■	■	■	■	■	■	■	■	■	■	■	■	■	■	■	■	■	■	■
G3									■	■	■	■	■	■	■									
G4								■	■	■	■	■	■	■	■									
G5						■	■	■	■	■	■	■	■	■	■	■	■	■	■	■	■			
G6									■	■	■	■	■					■	■	■	■			
G7						■				■	■	■								■	■	■		
G8					■		■					■								■				
G9				■				■				■								■				
G10			■																					

unit	Start and stop status of the unit every hour																							
	1	2	3	4	5	6	7	8	9	10	11	12	13	14	15	16	17	18	19	20	21	22	23	24
G1	■	■	■	■	■	■	■	■	■	■	■	■	■	■	■	■	■	■	■	■	■	■	■	■
G2	■	■	■	■	■	■	■	■	■	■	■	■	■	■	■	■	■	■	■	■	■	■	■	■
G3									■	■	■	■	■						■	■	■	■	■	
G4								■	■	■	■	■	■	■	■									
G5						■	■	■	■	■	■	■	■	■	■	■								
G6									■	■	■	■	■	■				■	■	■	■			
G7										■	■	■								■	■	■		
G8												■								■				
G9												■								■				
G10																								

Figure 8: Comparison between the unit combination calculated by the algorithm proposed in this paper and the original algorithm.

19 times is the theoretical optimal solution ($563937.7). The algorithm has strong stability and can converge to the optimal solution before the 5th generation in most cases. Table 5 lists the comparison between the convergence results of the algorithm in this paper and the traditional intelligent algorithm and its improved algorithm.

It can be seen that the algorithm generation and optimization mechanism proposed in this paper has high search quality and can quickly converge on the premise of ensuring that the search results meet various constraints of the power generation planning optimization model. The time is comparable, but the probability of finding a better solution is significantly improved.

5. Numerical Simulation Analysis of Wind Field

5.1. Sensitivity Analysis of Conditional Value-at-Risk Index in Single Period. Assuming that the units G1~G9 in the system are in the power-on state at a certain period of time, the total capacity of the thermal power units in the running state is 1607 MW, and the total installed capacity of the wind farms in the system is 400 MW. In order to analyze the influence of load and wind power output on the conditional value-at-risk index of power outage loss in a single period under a certain unit combination state, the power outage loss under different load levels and different wind power output levels was simulated by Monte Carlo, calculating the power balance risk measurement index for a single period. The parameters of the simulation calculation are set as follows: the minimum number of simulations is 1000 times, the maximum number of simulations is 5000 times, the confidence level is 0.95, and the unit compensation value coefficient for insufficient power is 1000$/MWh.

Figure 7 shows the comparison of the relationship between the value-at-risk of the single-period power outage loss condition and the positive spinning reserve capacity and the negative spinning reserve capacity: when the positive spinning reserve capacity is small, with the increase of the positive spinning reserve capacity, the power shortage conditional risk basically shows a linear decreasing trend, and when the positive spinning reserve capacity is greater than 600 MW, the conditional risk of power shortage is basically unchanged. At this time, increasing the spinning reserve capacity cannot reduce the economic risk loss. When the negative spinning reserve capacity is small, the conditional risk of peak shaving power abandonment loss is generally negatively correlated with the negative spinning reserve capacity. As the negative spinning reserve capacity increases, when the negative spinning reserve capacity is greater than 150 MW, the peak shaving conditional risk of wind curtailment loss is relatively small, and the risk of peak shaving and curtailment of wind farms can be ignored at this time.

5.2. Examples Analysis. In order to compare the optimization effect of the proposed algorithm, a wind farm with a total installed capacity of 420 MW is added to the original standard example system, accounting for about 25% of the total installed thermal power capacity of the system. The

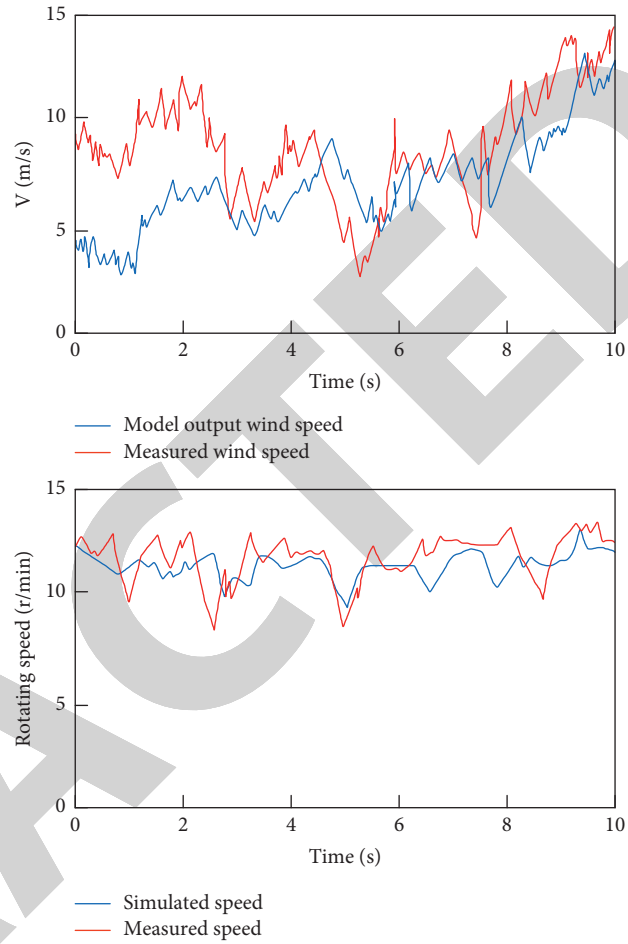

Figure 9: Simulation curves of measured rotor speed and wind speed during fan operation.

combination of units calculated by the algorithm proposed in this paper and the results obtained by the original algorithm are shown in Figure 8, in which the grey square indicates that the unit is in operation and the white square indicates that the unit is out of operation.

The total fuel cost of the original algorithm is $444,794, which is 21% lower than that before renewable energy is connected, and the start-stop cost is $6361, which is 55% higher than that before renewable energy is connected. It can be seen that although large-scale intermittent renewable energy access can reduce the total cost of power system dispatching and operation, it may lead to frequent startup and shutdown of conventional units and increase the startup and shutdown costs of units. The algorithm proposed in this paper is used to optimize the solution, and the variable neighborhood descent search algorithm optimization is enabled when the historical optimal solution after 5 iterations in the algorithm iteration process remains unchanged. The total fuel cost of the optimized solution is $444210, which is $584 less than the IPSO algorithm, and the start-stop cost is $5810, which is $551 less than the original algorithm.

5.3. Simulation Analysis. The left side of Figure 9 shows the measured wind speed during the operation of the front-end

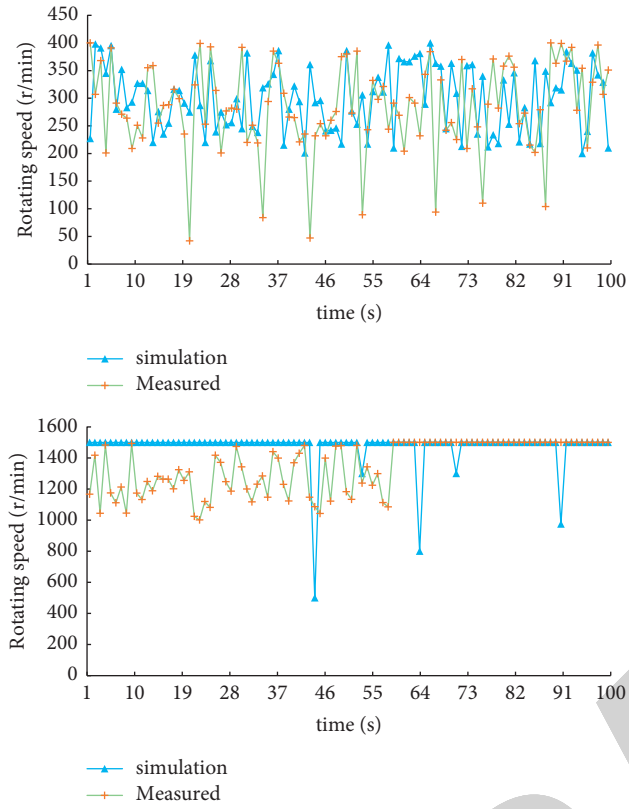

Figure 10: WinDrive input and output speed curve.

variable speed wind turbine and the wind speed curve simulated by the one-dimensional nonlinear wake model. The right side of Figure 9 shows the measured rotor speed and simulation output results during the operation of the fan.

It can be seen that due to the large fluctuation of the measured wind speed, the rotational speed of the wind rotor of the unit varies widely, but the rotational speed of the wind rotor can track the change of the wind speed in real time. It can also be seen from the simulation results that as the wind speed increases or decreases, the speed of the wind rotor realizes the tracking of the wind speed.

Figure 10 shows the WinDrive input speed simulation and measured curve, and Figure 10 shows the measured front-end speed-regulated wind turbine input speed and control simulation results during the operation of the unit.

As can be seen from the figure, when the actual wind speed is greater than the cut-in wind speed, the generator speed can always keep a constant value of 1500r/min due to the adjustment effect of the hydraulic speed-regulating gearbox WinDrive. When the wind speed is lower than the cut-in wind speed, the hydraulic torque converter guide vane control enables the generator to track the maximum speed so that it can be connected to the grid when the wind speed reaches the cut-in wind speed.

Based on the analysis, it can be concluded that the simulation control of wind speed can effectively control its economic risk after improvement, reduce the risk value by 24%, and reduce the economic cost by 8.66%. This shows that it has high practical application value.

6. Conclusions

This paper mainly studies the wind power generation system in renewable energy power generation. Through the relevant research on the wind speed in the wind power generation system and its control and understanding, it can be more efficient in the actual power generation effect. In addition, this paper conducts a detailed exploration and analysis of the modeling of wind power generation systems and fully understands the characteristics of renewable energy power generation, so that the modeling method proposed in this paper can be more targeted for wind speed modeling and analysis control. Finally, the experiment and analysis part are designed to explore its related performance, which not only ensures the efficiency but also ensures the stable operation of the system.

Data Availability

The data that support the findings of this study are available from the corresponding author upon reasonable request.

Conflicts of Interest

The authors declared no potential conflicts of interest with respect to the research, authorship, and/or publication of this article.

References

[1] T. Baležentis and D. Streimikiene, "Multi-criteria ranking of energy generation scenarios with Monte Carlo simulation," *Applied Energy*, vol. 185, no. 1, pp. 862–871, 2017.

[2] X. Xie, H. Liu, and J. He, "Small-signal impedance/admittance network modeling for grid-connected renewable energy generation systems," *Dianli Xitong Zidonghua/Automation of Electric Power Systems*, vol. 41, no. 12, pp. 26–32, 2017.

[3] H. Li, D. Chen, H. Zhang, and C. X. Wu, "Hamiltonian analysis of a hydro-energy generation system in the transient of sudden load increasing," *Applied Energy*, vol. 185, no. 1, pp. 244–253, 2017.

[4] F. J. Lozano and R. Lozano, "Assessing the potential sustainability benefits of agricultural residues: biomass conversion to syngas for energy generation or to chemicals production," *Journal of Cleaner Production*, vol. 172, no. 4, pp. 4162–4169, 2018.

[5] A. C. Lisboa, T. L. Vieira, L. S. M. Guedes, and D. A. G. R. R. Vieira, "Optimal analytic dispatch for tidal energy generation," *Renewable Energy*, vol. 108, no. AUG, pp. 371–379, 2017.

[6] C. Lohse, "Environmental impact by hydrogeothermal energy generation in low-enthalpy regions," *Renewable Energy*, vol. 128, no. PT, pp. 509–519, 2018.

[7] M. Rajarathinam and S. F. Ali, "Energy generation in a hybrid harvester under harmonic excitation," *Energy Conversion and Management*, vol. 155, no. JAN, pp. 10–19, 2018.

[8] K. N. Islam, "Municipal solid waste to energy generation: an approach for enhancing climate co-benefits in the urban areas of Bangladesh," *Renewable and Sustainable Energy Reviews*, vol. 81, no. 2, pp. 2472–2486, 2018.

[9] L. F. Morales-Mendoza and C. Azzaro-Pantel, "Bridging LCA data gaps by use of process simulation for energy generation,"

Clean Technologies and Environmental Policy, vol. 19, no. 5, pp. 1535–1546, 2017.

[10] E. Andenæs, B. P. Jelle, K. Ramlo, and T. J. S. E. Kolås, "The influence of snow and ice coverage on the energy generation from photovoltaic solar cells," *Solar Energy*, vol. 159, no. JAN, pp. 318–328, 2018.

[11] O. Bozorg-Haddad, I. Garousi-Nejad, and H. A. Loáiciga, "Extended multi-objective firefly algorithm for hydropower energy generation," *Journal of Hydroinformatics*, vol. 19, no. 5, pp. 734–751, 2017.

[12] S. O. Dahunsi, S. U. Oranusi, and V. E. Efeovbokhan, "Bioconversion of tithonia diversifolia (Mexican sunflower) and poultry droppings for energy generation: optimization, mass and energy balances, and economic benefits," *Energy & Fuels*, vol. 31, no. 5, pp. 5145–5157, 2017.

[13] Y. Xue, N. Chen, S. Wang, and F. Wen, "Review on wind speed prediction based on spatial correlation," *Dianli Xitong Zidonghua/Automation of Electric Power Systems*, vol. 41, no. 10, pp. 161–169, 2017.

[14] A. C. Sophia and S. Sreeja, "Green energy generation from plant microbial fuel cells (PMFC) using compost and a novel clay separator," *Sustainable Energy Technologies and Assessments*, vol. 21, no. jun, pp. 59–66, 2017.

[15] J. Kim, Y. Noh, and D. Chang, "Storage system for distributed-energy generation using liquid air combined with liquefied natural gas," *Applied Energy*, vol. 212, no. FEB.15, pp. 1417–1432, 2018.

[16] K. Benis, I. Turan, C. Reinhart, and P. Ferrão, "Putting rooftops to use - a Cost-Benefit Analysis of food production vs. energy generation under Mediterranean climates," *Cities*, vol. 78, no. AUG, pp. 166–179, 2018.

[17] S. Kamel, H. A. El-Sattar, D. Vera, and F. Jurado, "RETRACTED: b," *Renewable and Sustainable Energy Reviews*, vol. 94, no. OCT, pp. 28–37, 2018.

[18] A. P. Bernal, I. F. S. dos Santos, A. P. Moni Silva, and R. M. E. M. Barros, "Vinasse biogas for energy generation in Brazil: an assessment of economic feasibility, energy potential and avoided CO 2 emissions," *Journal of Cleaner Production*, vol. 151, no. MAY10, pp. 260–271, 2017.

[19] G. Xu, Z. Wang, J. Zhou et al., "Rotor loss and thermal analysis of synchronous condenser under single-phase short-circuit fault in the transmission line," *IEEE Transactions on Energy Conversion*, vol. 37, no. 1, pp. 274–285, 2022.

[20] A. S. Kocaman and V. Modi, "Value of pumped hydro storage in a hybrid energy generation and allocation system," *Applied Energy*, vol. 205, no. Nov.1, pp. 1202–1215, 2017.

[21] E. C. Rada, "Environmental pollution from waste and biomass energy generation," *International Journal of Energy Production and Management*, vol. 2, no. 1, pp. 1–7, 2017.

[22] Z. Lv, D. Chen, and Q. Wang, "Diversified technologies in internet of vehicles under intelligent edge computing," *IEEE Transactions on Intelligent Transportation Systems*, vol. 13, no. 99, pp. 1–12, 2020.

[23] Y. Li, Y. Zuo, H. Song, and Z. Lv, "Deep learning in security of internet of things," *IEEE Internet of Things Journal*, vol. 34, no. 99, p. 1, 2021.

[24] L. Zhang, H. M. Shi, X. H. Zeng, and Z. Zhuang, "Theoretical and experimental study on the transmission loss of a side outlet muffler," *Shock and Vibration*, vol. 2020, pp. 1–8, 2020.

[25] A. Iqbal and G. K. Singh, "PSO based controlled six-phase grid connected induction generator for wind energy generation," *CES Transactions on Electrical Machines and Systems*, vol. 5, no. 1, pp. 41–49, 2021.

[26] R. S. Parente, D. Alencar, P. Junior, I. Silva, and J. Liete, "Application OF the narx model for forecasting wind speed for wind energy generation," *International Journal of Development Research*, vol. 11, no. 4, pp. 46461–46466, 2021.